Inertial Lévy flight

Yan Lü and Jing-Dong Bao*
Department of Physics, Beijing Normal University, Beijing 100875, People's Republic of China
(Received 9 August 2011; published 11 November 2011)

Lévy flights with inertial term in various potentials are studied analytically and numerically in terms of the fractional Fokker-Planck equation. The probability density functions of the Lévy flight particle in the linear and harmonic potentials are exactly obtained and a transient contribution of inertial term is found in the case of linear potential, which can be neglected when evolution time is much longer than γ^{-1} (γ is the damping coefficient); for the harmonic potential, where the stationary state has still infinite variance of coordinate and its width is larger than that of the inertialess case for arbitrary Lévy index μ in the region of $0 < \mu < 2$, we still find that the distribution of velocity of the particle is also the Lévy-type one. Moreover, a crossover from bimodal to unimodal shape for the spatial distribution is shown in the anharmonic potential. Finally, we represent an analytical expression of the rate constant for the inertial Lévy flight particle escaping from a metastable potential by using the reactive flux method and show that the rate is a nonmonotonic function of the Lévy index.

DOI: 10.1103/PhysRevE.84.051108 PACS number(s): 05.40.Fb, 02.50.Ey, 05.40.Ca

I. INTRODUCTION

Anomalous diffusion and its phenomena have been attracting growing interest. The mean square displacement of a force-free particle in the long time reads $\langle x^2(t)\rangle \propto t^\alpha$, where $0 < \alpha < 1$ is subdiffusion, $\alpha = 1$ is normal diffusion, and $1 < \alpha < 2$ is superdiffusion. Prominent examples of subdiffusion include charge carrier transport in amorphous semiconductors [1], the motion of beads in actin gels [2], and chaotic maps [3]. The superdiffusion was found in layered velocity field [4]. For the description of anomalous diffusion, several approaches have been developed [1,5,6] whereby a surprise superdiffusive motion is induced in the Lévy flight.

The Lévy flight has been used to model various processes such as self-diffusion in micelle systems [7], special problems in reaction dynamics [8], and even the flight of an albatross [9]. They are characterized by the occurrence of extremely long jumps which are associated with a complex structure of the environment, in particular with long-range correlation. The jump length is sampled according to the Lévy stable statistics with a power law tail of the form: $\sim|x|^{-\mu-1}$, where μ is the Lévy index taking value in the region of $0 < \mu < 2$, which leads to the divergent of the second moment of the coordinate of the particle even in a harmonic potential [10]. This kind of peculiar property strongly contradicts the ordinary Brownian motion. An impressive experimental evidence of Lévy flight was reported in the single-ion motion in a one-dimensional optical lattice, in which the diverging fluctuation was observed in the kinetic energy [11]. As one knows, the understanding of stochastic processes comes from their behavior in various external potentials. The Langevin equation driven by a white Lévy noise provides a basis for Lévy flight. Alternatively, the probability density function of Lévy flight obeys the fractional Fokker-Planck equation (FFPE). It is noticed that the distribution of the particle with infinite variance in the harmonic potential is given by a unimodal Lévy stable law which exhibits the non-Boltzmann nature [10]. If the Lévy flight particle is in a steeper potential $U(x) \sim \frac{x^{2n+2}}{2n+2}(n = 1,2,\ldots)$, its spatial distribution displays a distinct bimodal character and variance is finite. In particular, the stable Lévy noise induces a crossover from unimodal to bimodal behavior of the particle in anharmonic potential [12].

Nevertheless, all the above studies are limited to the overdamping cases. In practice, many systems in physics, chemistry, and biology are environment dependent; namely, the particle may experience weak damping. In order to describe the motion of a general damping particle driven by white Lévy noise, one needs to consider the inertial term. Since the variance of the Lévy noise is divergent, an infinite amount of energy cannot be balanced by the dissipation [13]. In fact, the Lévy noise can only be seen as an external one which is produced by a process and independent of the damping [14].

In this work we study analytically and numerically the novel behaviors of Lévy flight with inertial terms. The paper is organized as follows. In Sec. II, after a brief introduction of the model for the inertial Lévy flight, we get the exact expressions of the probability density function of a particle in linear and harmonic potentials by solving the FFPE and the results are presented. In Sec. III, we consider an inertial Lévy flight particle escaping from a metastable potential and calculate the stationary escape rate based on the reactive flux method. A summary is given in Sec. IV.

II. THE STABLE BEHAVIORS OF INERTIAL LÉVY FLIGHT

The dynamics of a particle under the influence of an external potential $U(x)$ and a white Lévy noise $\xi(t)$ is defined as follows:

$$\dot{x} = v, \dot{v} = -\gamma v + \frac{F(x)}{m} + \frac{\xi(t)}{m}, \tag{1}$$

where $F(x) = -U'(x)$, m is the mass of the particle, γ denotes the damping coefficient, and $\xi(t)$ is the zero-mean white Lévy noise. In the Fourier space, one defines the characteristic function $p(k)$ of the Lévy noise,

$$p(k) = \int_{-\infty}^{\infty} \exp(-ik\xi)p(\xi)d\xi = \exp(-D|k|^\mu), \tag{2}$$

*jdbao@bnu.edu.cn

where the parameter D measures the intensity of Lévy noise. In the presence of such noise, we arrive at the FFPE [15] corresponding to Eq. (1):

$$\frac{\partial W(x,v,t)}{\partial t} = -v\frac{\partial W(x,v,t)}{\partial x} + \gamma\frac{\partial [vW(x,v,t)]}{\partial v} - \frac{F(x)}{m}\frac{\partial W(x,v,t)}{\partial v} + \frac{D}{m^{\mu}}\frac{\partial^{\mu} W(x,v,t)}{\partial |v|^{\mu}}. \quad (3)$$

The Riesz fractional derivative in Eq. (3) is defined through its Fourier transform,

$$-\frac{\partial^{\mu}}{\partial |v|^{\mu}} = \frac{1}{2\pi}\int_{-\infty}^{\infty} dk_2 \exp(-ik_2 v)|k_2|^{\mu}. \quad (4)$$

In the following we analyze the probability density function of the particle under the linear, harmonic, and quartic potentials, respectively.

A. Linear potential

We consider first the linear potential case: $U(x) = -F_0 x$ and then $F(x) = F_0$ in Eq. (3). If one knows the solution of the FFPE (3), the probability density function of the coordinate can be obtained through integrating over the velocity variable v:

$$W(x,t) = \int_{-\infty}^{\infty} W(x,v,t)dv. \quad (5)$$

Using the Fourier transformation for Eq. (3) with respect to both x and v, the equation of the characteristic function $\tilde{W}(k_1,k_2,t)$ is given by

$$\frac{\partial \tilde{W}(k_1,k_2,t)}{\partial t} - (k_1 - \gamma k_2)\frac{\partial \tilde{W}(k_1,k_2,t)}{\partial k_2} = -\frac{ik_2 F_0}{m}\tilde{W}(k_1,k_2,t) - \frac{D}{m^{\mu}}|k_2|^{\mu}\tilde{W}(k_1,k_2,t). \quad (6)$$

To solve the above equation by the characteristics method, we put it into the form

$$\frac{1}{(ik_2 F_0 m^{\mu-1} D^{-1} + |k_2|^{\mu})}\frac{\partial \tilde{W}(k_1,k_2,t)}{\partial t} - \frac{(k_1 - \gamma k_2)}{(ik_2 F_0 m^{\mu-1} D^{-1} + |k_2|^{\mu})}\frac{\partial \tilde{W}(k_1,k_2,t)}{\partial k_2} = -\frac{D}{m^{\mu}}\tilde{W}(k_1,k_2,t). \quad (7)$$

Equation (7) is the first-order linear partial differential equation for t and k_2, since k_1 can be regarded as a parameter. The characteristic equation of Eq. (7) can be written as a set of equations:

$$\frac{dt}{ds} = \frac{1}{(ik_2 F_0 m^{\mu-1} D^{-1} + |k_2|^{\mu})}, \quad \frac{dk_2}{ds} = -\frac{(k_1 - \gamma k_2)}{(ik_2 F_0 m^{\mu-1} D^{-1} + |k_2|^{\mu})}, \quad \frac{d\tilde{W}(k_1,k_2,t)}{ds} = -Dm^{-\mu}\tilde{W}(k_1,k_2,t), \quad (8)$$

with the initial conditions $t(0) = 0$, $k_2(0) = r$, and $\tilde{W}(k_1,k_2,0) = 1$. The third initial condition reflects the requirement that $W(x,v,0)$ is a δ function for the variables x and v. Combining the first two equations of Eq. (8) and taking account of the initial conditions, we get the relation between k_2 and t on the characteristic curve,

$$k_2(r,t) = \left(r - \frac{k_1}{\gamma}\right)e^{\gamma t} + \frac{k_1}{\gamma}, \quad (9)$$

and the function of r is therefore determined by

$$r(k_2,t) = \frac{k_1}{\gamma} + \left(k_2 - \frac{k_1}{\gamma}\right)e^{-\gamma t}. \quad (10)$$

The Fourier transform of Eq. (5) is

$$\tilde{W}(k_1,t) = \int_{-\infty}^{\infty} W(x,t)\exp(-ik_1 x)dx = \int_{-\infty}^{\infty}\int_{-\infty}^{\infty} W(x,v,t)dv\exp(-ik_1 x)dx = \tilde{W}(k_1,k_2 = 0,t) = \exp[-Dm^{-\mu}s(k_2 = 0,t)]. \quad (11)$$

Here we have used the expressions of $s(k_2,t)$ and $\tilde{W}(k_1,k_2,t)$, which are derived by integrating the second and third equations in (8):

$$s(k_2,t) = \int_r^{k_2}\left[\frac{ik_2' F_0 m^{\mu-1}}{D(\gamma k_2' - k_1)} + \frac{|k_2'|^{\mu}}{(\gamma k_2' - k_1)}\right]dk_2', \quad (12)$$

$$\tilde{W}(k_1,k_2,t) = \exp(-Dm^{-\mu}s). \quad (13)$$

Inserting Eq. (10) into Eq. (11), and replacing some variables, we eventually get

$$\tilde{W}(k_1,t) = \exp[-i\sigma_1(t)k_1 - D\sigma_2(t)|k_1|^{\mu}], \quad (14)$$

where

$$\sigma_1(t) = \frac{F_0}{m\gamma^2}\int_0^g \frac{k_2'}{(1-k_2')}dk_2' = \frac{F_0}{m\gamma^2}(e^{-\gamma t} - 1) + \frac{F_0 t}{m\gamma}, \quad \sigma_2(t) = \frac{1}{m^{\mu}\gamma^{\mu+1}}\int_0^g \frac{(k_2')^{\mu}}{(1-k_2')}dk_2' = \frac{1}{m^{\mu}\gamma^{\mu+1}}B_g(\mu+1,0), \quad (15)$$

and $g(t) = 1 - e^{-\gamma t}$. $B_z(a,b) = \int_0^z t^{a-1}(1-t)^{b-1}dt$ is the incomplete β function.

The parameter $\sigma_2(t)$ in Eq. (14) can be exactly evaluated if μ is a rational number. For instance, for $\mu = \frac{1}{2}$, $\mu = 1$, and $\mu = \frac{3}{2}$, it yields

$$\mu = \frac{1}{2}, \quad \sigma_2(t) = \frac{1}{m^{\frac{1}{2}}\gamma^{\frac{3}{2}}}\left[-2\sqrt{1-e^{-\gamma t}} + \ln\left(\frac{-1-\sqrt{1-e^{-\gamma t}}}{-1+\sqrt{1-e^{-\gamma t}}}\right)\right],$$

$$\mu = 1, \quad \sigma_2(t) = \frac{1}{m\gamma^2}(e^{-\gamma t} - 1) + \frac{t}{m\gamma},$$

$$\mu = \frac{3}{2}, \quad \sigma_2(t) = \frac{m}{m^{\frac{3}{2}}\gamma^{\frac{5}{2}}}\left[-2\sqrt{1-e^{-\gamma t}} - \frac{2}{3}(1-e^{-\gamma t})^{\frac{3}{2}} + \ln\left(\frac{-1-\sqrt{1-e^{-\gamma t}}}{-1+\sqrt{1-e^{-\gamma t}}}\right)\right]. \quad (16)$$

In the limit of $\gamma t \to \infty$, $\sigma_2(t)$ can be approximated by $\sigma_2(t) \approx \frac{t}{m^{\mu}\gamma^{\mu}}$. In comparison with Eq. (2), we find that Eq. (14) is the characteristic function of the Lévy distribution, but in the

translated coordinate $\sigma_1(t)$, the probability density function in Eq. (5) is determined from the inverse Fourier transform of $\tilde{W}(k_1,t)$:

$$\begin{aligned} W(x,t) &= \frac{1}{2\pi}\int_{-\infty}^{\infty}\tilde{W}(k_1,t)\exp(ik_1x)dk_1 \\ &= (D\sigma_2(t))^{-\frac{1}{\mu}}L_\mu\left(\frac{|x-\sigma_1(t)|}{(D\sigma_2(t))^{\frac{1}{\mu}}}\right) \\ &= \frac{\pi}{\mu|x-\sigma_1(t)|}H_{2,2}^{1,1} \\ &\quad\times\left[\frac{|x-\sigma_1(t)|}{(D\sigma_2(t))^{\frac{1}{\mu}}}\middle|\begin{matrix}(1,1/\mu), & (1,1/2)\\ (1,1), & (1,1/2)\end{matrix}\right], \end{aligned} \tag{17}$$

where $H_{2,2}^{1,1}$ is Fox's H function. The asymptotic behavior of the $W(x,t)$ reads

$$W(x,t)\sim\frac{D\sigma_2(t)}{|x|^{\mu+1}}, \tag{18}$$

which should lead to divergence of the mean square displacement of a particle if $\mu\neq 2$. The displacement of the particle is due to the balancing of the friction against the imposed constant force, that is, $x(t)=\sigma_1(t)=\frac{F_0}{m\gamma^2}(e^{-\gamma t}-1)+\frac{F_0t}{m\gamma}$. It shows a transient contribution of the inertial term. In this case, if the first moment exists, that is, for $1<\mu\leqslant 2$, we find from Eq. (14) the average of the coordinate of particle $\langle x(t)\rangle=\sigma_1(t)$. In the limit of $\gamma t\to\infty$, $\sigma_1(t)=\frac{F_0t}{m\gamma}$, and $\sigma_2(t)=\frac{t}{m^\mu\gamma^\mu}$, the role of the inertial term disappears, we go directly to the steady state described by $\gamma mv=F_0$, and the Lévy flight in a constant force field is equivalent to the motion in a constant velocity field. The steady state depends on both μ and γ and the convergence is fast for small μ and large γ.

When $F_0=0$, the shift of the distribution vanishes and Eq. (17) reduces into the result of the force-free case,

$$W(x,t)=\frac{\pi}{\mu|x|}H_{2,2}^{1,1}\left[\frac{|x|}{(D\sigma_2(t))^{\frac{1}{\mu}}}\middle|\begin{matrix}(1,1/\mu), & (1,1/2)\\ (1,1), & (1,1/2)\end{matrix}\right]. \tag{19}$$

The mean square displacement of the particle is finite for the special case $\mu=2$, which corresponds to the usual Brownian behavior. In the general case of $0<\mu<2$, when the transient contribution of the inertial term disappears, the width of distribution $\sigma_2(t)$ coincides with the solution of the overdamping case $\gamma\to\infty$, and the scaling result in an imaginary growing box is $\langle x^2(t)\rangle_L\sim\int_{-Lt^{1/\mu}}^{Lt^{1/\mu}}x^2W(x,t)dx\sim t^{2/\mu}$.

Using the Laplace transform technique, the formal expression for the solution of Eq. (1) can be written as

$$\begin{aligned} x(t) &= \frac{F_0t}{m\gamma}+\frac{F_0}{m\gamma^2}(e^{-\gamma t}-1) \\ &\quad+\frac{1}{m\gamma}\int_0^t(1-e^{-\gamma(t-t')})\xi(t')dt'. \end{aligned} \tag{20}$$

From Eq. (20), we see that for a constant force, the particle is accelerated before reaching the steady state with a constant velocity $v=\frac{F_0}{m\gamma}$. In the accelerating process, the inertial term plays a role and the damping effect is important. For very long times, the velocity of the particle approaches a constant value, the inertial effect disappears, and a steady state is reached.

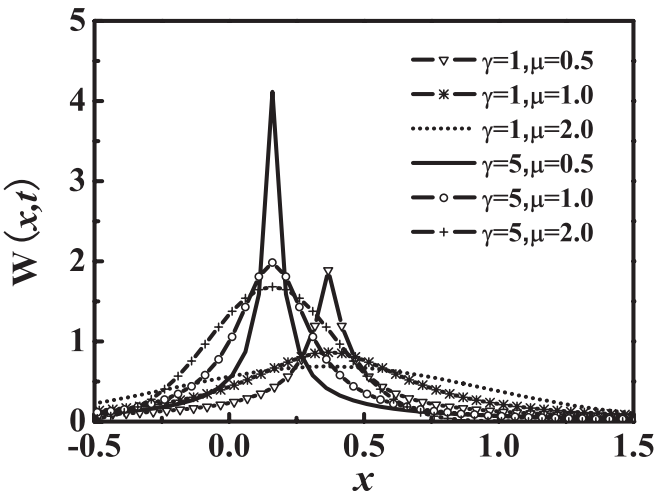

FIG. 1. The probability density function of the coordinate of constant-force particle at time $t=1.0$. The parameters used are $F_0=1.0$, $m=1.0$, and $D=1.0$.

Figure 1 shows the distribution of coordinates of the particle at $t=1.0$ under the external force $F_0=1.0$. For finite times, the effect of the inertial term is not negligible. In comparison with the overdamping case, both the width and the shift of the distribution of coordinates are small.

In order to see the transient contribution of the inertial term, in Fig. 2, we plot the rescaled parameter quantities:

$$\theta_1(t)=\frac{\sigma_1(t)}{F_0t/m\gamma}, \tag{21}$$

$$\theta_2(t)=\frac{\sigma_2(t)}{t/m^\mu\gamma^\mu}. \tag{22}$$

For small times, the transient effect of the inertial term is obvious for different values of γ. However, when time is much longer than the characteristic time γ^{-1}, the inertial effect can be neglected, both $\theta_1(t)$ and $\theta_2(t)$ converge to 1, and then $\sigma_1(t)$ and $\sigma_2(t)$ have the same forms as the overdamping case. It is obvious that the time needed for the particle to converge to the steady state increases with the increase of μ and the decrease of γ.

On the other hand, we also obtain the velocity distribution function $W(v,t)$ of the particle, which is defined as

$$W(v,t)=\int_{-\infty}^{\infty}W(x,v,t)dx; \tag{23}$$

then the characteristic function $\tilde{W}(k_2,t)$ can be written as

$$\begin{aligned} \tilde{W}(k_2,t) &= \int_{-\infty}^{\infty}W(v,t)\exp(-ik_2v)dv \\ &= \int_{-\infty}^{\infty}\int_{-\infty}^{\infty}W(x,v,t)dx\exp(-ik_2v)dv \\ &= \tilde{W}(k_1=0,k_2,t). \end{aligned} \tag{24}$$

Taking account of Eqs. (12) and (13), we eventually get

$$\tilde{W}(k_2,t)=\exp[-i\beta_1(t)k_2-D\beta_2(t)|k_2|^\mu], \tag{25}$$

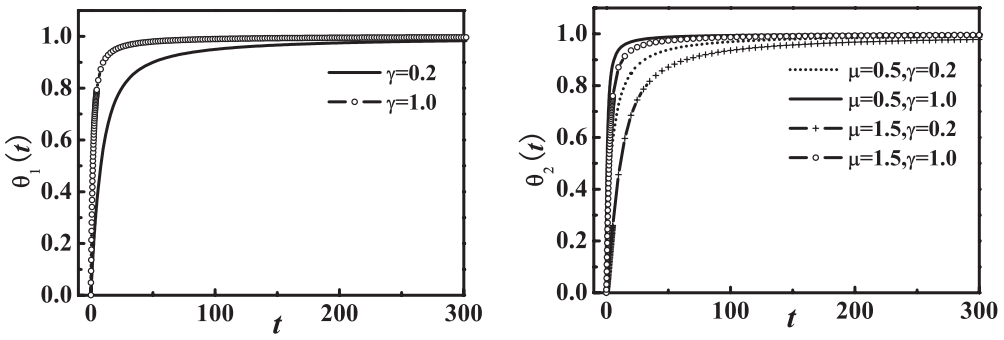

FIG. 2. The rescaled shift of the coordinate $\theta_1(t)$ [Eq. (21)] and the rescaled width of coordinate distribution $\theta_2(t)$ [Eq. (22)] versus time. The parameters used are $F_0 = 1.0$, $m = 1.0$, and $D = 1.0$.

where

$$\beta_1(t) = \frac{F_0}{\gamma m}(1 - e^{-\gamma t}),$$
$$\beta_2(t) = \frac{1}{m^\mu \mu\gamma}(1 - e^{-\gamma\mu t}). \tag{26}$$

In fact, Eq. (25) is the characteristic function of Lévy distribution, its shift and width are determined by $\beta_1(t)$ and $\beta_2(t)$, respectively. In the limit of $t \to \infty$, both the shift and the width of the velocity distribution always approach constants. This means that the distribution of velocity can converge to the steady state in the long-time limit.

In Fig. 3, we plot the velocity distribution of the particle at $t = 1.0$ and $t = 10.0$ (a steady state). The asymptotic behavior of the velocity distribution reads $W(v) \sim \frac{D\beta_2(t)}{|v|^{1+\mu}}$, which leads to divergence of the variance of velocity. Then we must calculate the steady variance of velocity in a fix box. When $F_0 = 0$, we have

$$\langle v^2\rangle_L = \int_{-L}^{L} W(v)v^2 dv \sim \frac{2D}{m^\mu\mu\gamma}\frac{L^{2-\mu}}{(2-\mu)} \tag{27}$$

for the stationary velocity distribution, where L is the length of the box. It is obvious that the variance of velocity also depends on L.

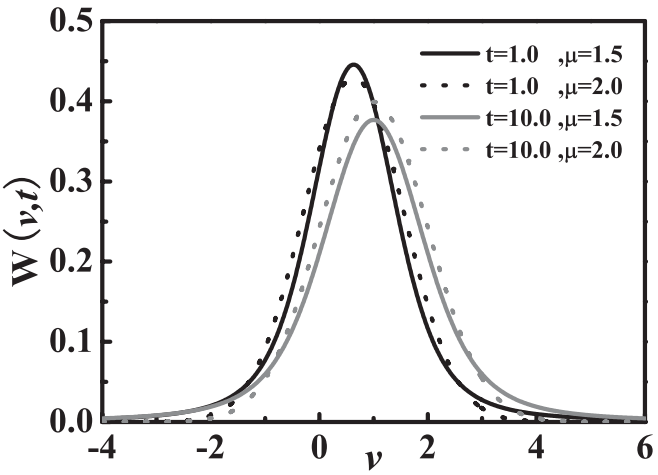

FIG. 3. The velocity distribution of the particle Eq. (23) in the constant force field. The parameters used are $F_0 = 1.0$, $\gamma = 1.0$, $m = 1.0$, and $D = 1.0$.

B. Harmonic potential

For the harmonic potential $U(x) = \frac{1}{2}m\omega^2 x^2$, the conjugate equation in the Fourier space, which corresponds to the FFPE (3), reads

$$\frac{\partial\tilde{W}(k_1,k_2,t)}{\partial t} - (k_1 - \gamma k_2)\frac{\partial\tilde{W}(k_1,k_2,t)}{\partial k_2} + \omega^2 k_2\frac{\partial\tilde{W}(k_1,k_2,t)}{\partial k_1}$$
$$= -Dm^{-\mu}|k_2|^\mu\tilde{W}(k_1,k_2,t). \tag{28}$$

Due to the symmetry of $\tilde{W}(k_1,k_2,t)$ for k_1, we consider the positive semiaxis, $k_1 \geqslant 0$. We try to find the solution in the same form as the Lévy distribution. With the transformation $k_2 = Kk_1$, we write the solution of the above equation as

$$\tilde{W} = \exp[-D|k_1|^\mu f(K,t)]. \tag{29}$$

As $k_2 = 0, K = 0$, the Fourier transform of $W(x,t)$ is given by

$$\tilde{W}(k_1,t) = \tilde{W}(k_1,k_2 = 0,t) = \exp[-D|k_1|^\mu f(t)]. \tag{30}$$

It is a Lévy distribution with the width $f(t)$. Substituting Eq. (29) into Eq. (28), we yield the equation of $f(K,t)$

$$\frac{\partial f}{\partial t} - (\omega^2K^2 - \gamma K + 1)\frac{\partial f}{\partial K} = m^{-\mu}|K|^\mu - \omega^2\mu K f, \tag{31}$$

with the initial condition $f(K,t = 0) = 0$, which can be obtained from $\tilde{W}(k_1,k_2,t = 0) = 1$. When $K = 0$, the width of distribution $f(t)$ in Eq. (30), following Eq. (A7), takes the form

$$f(t) = \int_0^t g(K = 0,t - s)ds = \int_0^t |c_0(t - s)|^\mu ds, \tag{32}$$

where

$$c_0(t) = \begin{cases} \frac{2}{m\sqrt{\gamma^2-4\omega^2}}e^{-\frac{\gamma t}{2}}\sinh\left(\frac{t}{2}\sqrt{\gamma^2-4\omega^2}\right), & \text{for } \gamma > 2\omega, \\ \frac{2}{m\sqrt{4\omega^2-\gamma^2}}e^{-\frac{\gamma t}{2}}\sin\left(\frac{t}{2}\sqrt{4\omega^2-\gamma^2}\right), & \text{for } \gamma < 2\omega, \\ \frac{t}{m}e^{-\frac{\gamma t}{2}}, & \text{for } \gamma = 2\omega. \end{cases} \tag{33}$$

Then the characteristic function of $W(x,t)$ can be presented in the form

$$\tilde{W}(k_1,t) = \exp\left(-D|k_1|^\mu\int_0^t |c_0(t - s)|^\mu ds\right). \tag{34}$$

This is always the characteristic function of Lévy distribution with the power index μ. Note that this shape is the same as the driven white Lévy noise, only with a different

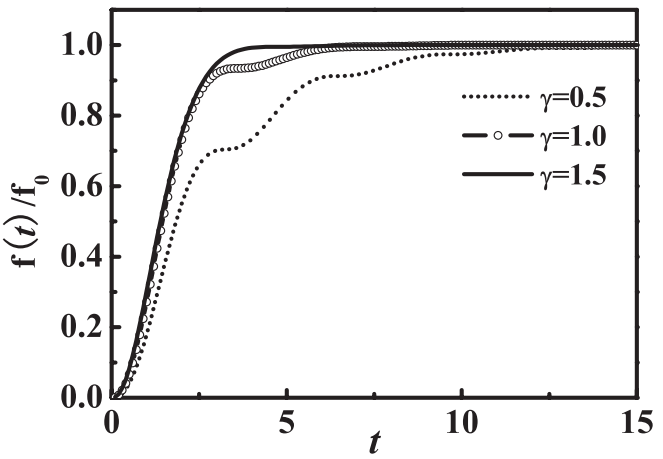

FIG. 4. Time evolution of the rescaled width of distribution $f(t)/f_0$ [Eq. (37)]. The parameters used are $\mu = 1.5$, $\omega^2 = 1.0$, $m = 1.0$, and $D = 1.0$.

"width" $D \to D\int_0^t |c_0(t-s)|^\mu ds$. For $\mu = 2$, the Brownian result with a finite variance is recovered, but in the general case $0 < \mu < 2$, an entirely different case arises. In the limit of $t \to \infty$, we always reach the characteristic function of the stationary distribution

$$\tilde{W}_{\rm st}(k_1) = \exp(-D|k_1|^\mu f_0), \tag{35}$$

where $f_0 = \int_0^\infty |c_0(t)|^\mu dt$. The exact stationary solution in the coordinate space can be written in terms of Fox's H function:

$$W_{\rm st}(x) = \frac{\pi}{\mu|x|} H_{2,2}^{1,1}\left[\frac{|x|}{(Df_0)^{\frac{1}{\mu}}}\middle|\begin{matrix}(1,1/\mu), & (1,1/2)\\ (1,1), & (1,1/2)\end{matrix}\right]$$
$$= \frac{\pi}{|x|} H_{2,2}^{1,1}\left[\frac{|x|^\mu}{Df_0}\middle|\begin{matrix}(1,1), & (1,\mu/2)\\ (1,\mu), & (1,\mu/2)\end{matrix}\right]. \tag{36}$$

This leads to the asymptotic power-law behavior $W_{st}(x) \sim \frac{Df_0}{|x|^{1+\mu}}$. It is seen that only in the case of $\mu = 2$, we recover the Boltzmann distribution $W(x) \propto e^{-\frac{\gamma m^2\omega^2 x^2}{2D}}$.

Now we give some remarks about the Langevin equation (1). If the damping coefficient is small, the inertial effect is obvious. Via the damping term $-\gamma m\dot{x}$ the finite energy of the particle is dissipated into the surrounding environment while the environment provides an infinite amount of energy through the Lévy noise. Then the particle takes a long time to reach a stationary state. In the extreme case, $\gamma \to 0$, the effect of the damping term can be neglected, the particle never reaches a stationary state. With the increase of the damping coefficient γ, the inertial effect becomes negligible, then the particle behaves as in the overdamping case.

From Eq. (33), we see that the inertial effect becomes significant when $\gamma < 2\omega$, for which the distribution width shows an oscillatory behavior for finite time. To show this phenomenon in detail, we plot the time evolution of the rescaled width

$$\frac{f(t)}{f_0} = \frac{\int_0^t |c_0(t-s)|^\mu ds}{\int_0^\infty |c_0(t')|^\mu dt'}, \tag{37}$$

for various γ in Fig. 4. Besides, it is obvious that the particle needs more time to relax to a stationary state if the damping coefficient is small.

The profiles of the stationary distributions for the coordinate of particle in the harmonic potential are shown in Fig. 5(a).

For general case $0 < \mu < 2$, $W(x)$ has a power-law tail and possesses no finite variance. This is the consequence of the energy supplied by the white Lévy noise, which cannot be balanced by the dissipation. At the same time, the width of the stationary distribution is influenced by the inertial term. To show this, in Fig. 5(b), we plot the rescaled width $\kappa(\gamma)$ as a function of γ, where $\kappa(\gamma)$ is defined as

$$\kappa(\gamma) = \frac{f_0}{f_{\rm over}}, \tag{38}$$

where $f_{\rm over} = 1/(\mu\omega^2 m^\mu \gamma^{\mu-1})$ is the width of steady distribution in the overdamping case. Noticed that for $\mu = 2$, the width keeps the same form as $f_{\rm over}$. However, for $0 < \mu < 2$, a different situation arises. It is obvious that when γ is small, f_0 deviates from $f_{\rm over}$. With the increase of γ, the width converges to the overdamping result when the inertial effect becomes negligible.

In Eq. (23), we have given the distribution of the velocity. Taking account of Eqs. (29) and (A7), the characteristic function of the velocity distribution $\tilde{W}(k_2,t)$ can be written as

$$\tilde{W}(k_2,t) = \exp\left[-D|k_2|^\mu \int_0^t |c_1(t-s)|^\mu ds\right], \tag{39}$$

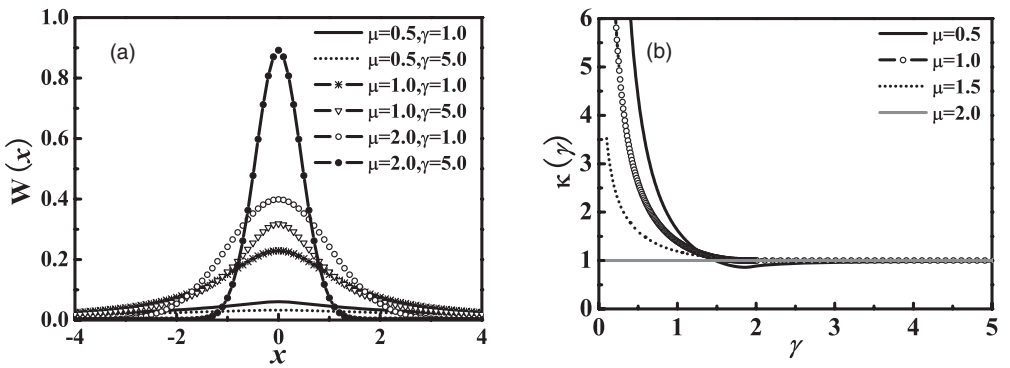

FIG. 5. (a) The stationary distribution of coordinate the harmonic particle Eq. (36). (b) Rescaled width of distribution $\kappa(\gamma)$ [Eq. (38)]. The parameters used are $\omega^2 = 1.0$, $m = 1.0$, and $D = 1.0$.

where

$$c_1(t) = \begin{cases} \frac{1}{m\sqrt{\gamma^2-4\omega^2}} e^{-\frac{\gamma t}{2}} \left[-\gamma \sinh\left(\frac{t}{2}\sqrt{\gamma^2-4\omega^2}\right) + \sqrt{\gamma^2-4\omega^2}\cosh\left(\frac{t}{2}\sqrt{\gamma^2-4\omega^2}\right)\right], & \text{for} \quad \gamma > 2\omega, \\ \frac{1}{m\sqrt{4\omega^2-\gamma^2}} e^{-\frac{\gamma t}{2}} \left[-\gamma \sin\left(\frac{t}{2}\sqrt{4\omega^2-\gamma^2}\right) + \sqrt{4\omega^2-\gamma^2}\cos\left(\frac{t}{2}\sqrt{4\omega^2-\gamma^2}\right)\right], & \text{for} \quad \gamma < 2\omega, \\ \frac{1}{m} e^{-\frac{\gamma t}{2}}\left(1-\frac{\gamma t}{2}\right), & \text{for} \quad \gamma = 2\omega. \end{cases} \tag{40}$$

It is obvious that it keeps Lévy shape for $0 < \mu < 2$. The velocity distribution reaches stationary in the limit of $t \to \infty$. In this case, $\tilde{W}(k_2)$ can be written as

$$\tilde{W}(k_2) = \exp\left[-D|k_2|^\mu \int_0^\infty |c_1(s)|^\mu ds\right]. \tag{41}$$

In Fig. 6, we present the stationary velocity distribution of the particle in the harmonic potential.

When $\mu = 2$, $W(v) \propto e^{-\frac{\gamma m^2 v^2}{2D}}$, then the variance of the velocity is finite. For the general case $0 < \mu < 2$, we give the variance in a fix box:

$$\langle v^2 \rangle_L \sim 2D \int_0^\infty |c_1(s)|^\mu ds \frac{L^{2-\mu}}{(2-\mu)}. \tag{42}$$

C. Quartic potential

We now consider the inertial Lévy flight in the quartic potential $U(x) = \frac{1}{4}mx^4$. It is complicated to solve the FFPE in practice, so we determine the probability density function by simulating the stochastic trajectories numerically from Eq. (1). For that purpose, the stochastic Euler algorithm is applied (see Appendix B).

Previous work has shown that the spatial distribution of Lévy flight particle presents a bimodality shape in a quartic potential for any $\mu \in (0,2)$ without the inertial term [12]. The presence of two maxima is a peculiarity of the Lévy flight. Due to the extremely long jumps, the particle driven by Lévy noise reaches very quickly to the region near the potential wall on both sides of the origin $x = 0$. Then it spends a long time to diffuse around this position, until a new long jump in the opposite motion moves it to reach the other side of the potential. That means the quartic potential can capture the particle in some symmetric areas with respect to $x = 0$; in this case, it is equivalent to the existence of two wells on the both side of the coordinate $x = 0$, and the stationary distribution has two humps. However, if the inertial term in the Langevin equation is included, an entirely different case should arise.

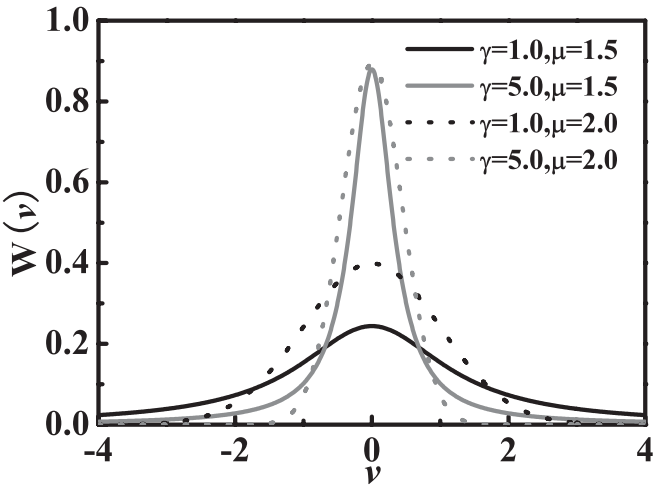

FIG. 6. The stationary velocity distributions for the harmonically bounded particle. The parameters used are $\omega^2 = 1.0$, $m = 1.0$, and $D = 1.0$.

In Fig. 7(a), we present the stationary distribution of the coordinate of particle with Lévy index $\mu = 1$ for various values of γ. There is a turnover from bimodality to unimodality as γ decreases. It indicates that when γ increases, the bimodality is most pronounced. With γ decreasing, the bimodality becomes weak, and it vanishes at a proper value of γ_c. In other words, the appearance of the bimodality becomes difficult when the inertial term is included. The reason is explained as follows. When γ is small and the inertial effect of the particle is obvious, we say that the particle is "heavy." Under the influence of the external Lévy noise, the inertial effect decreases the jump length of the particle; then the probability for the occurrence of extremely long jump of the particle is reduced, so it is difficult for the potential to capture the "heavy" particle on both sides of the origin point.

In this process, the inertial effect of particle reduces its probability for the occurrence of an extremely long jump; on the other hand, the long tail of the white Lévy noise makes the long jump occur frequently. The competition of the inertial effect and the long tail of noise distribution is the origin of the transition between bimodality and unimodality.

In Fig. 7(b), we plot a phase diagram which shows bimodal-unimodal transition of the stationary distribution. It is seen that the transition between bimodal and unimodal happens easily when the value of μ is large. That is because the increase of the Lévy index μ also decreases the probability for the long jump of the particle; that is, it acts in the analogous ways to decrease the damping strength.

III. THE ESCAPE RATE OF LÉVY FLIGHT IN A METASTABLE POTENTIAL

Finally, we use the reactive flux method [16,17] to derive the expression of rate constant for the inertial Lévy flight in a metastable potential, where the initial condition of the particle is assumed at the top of the barrier. The starting point for the method of reactive flux is the expression for the rate constant [17]

$$k(t) = \frac{\langle v_0 \delta(x_0) \theta_p[x(x_0, v_0, t)]\rangle}{\langle \theta_R(x_0)\rangle}, \tag{43}$$

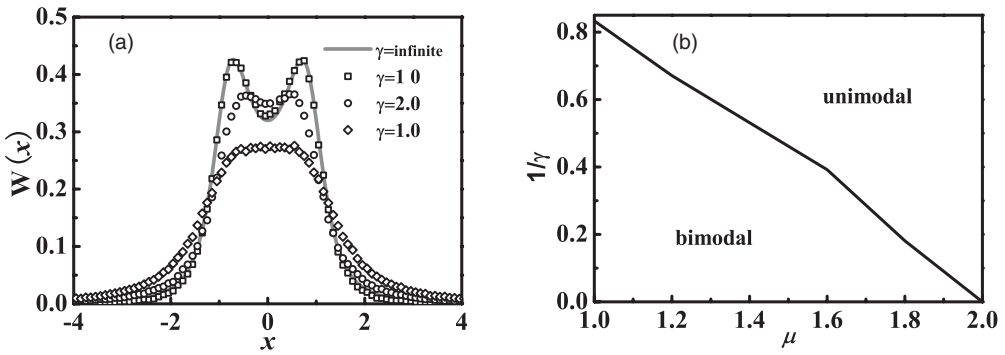

FIG. 7. (a) The stationary coordinate distribution of the particle in the quartic potential. (b) The phase diagram which shows the bimodal-unimodal transition of the coordinate distribution of the particle in such potential. The parameters used are $m = 1.0$ and $D = 1.0$.

where $\theta_R[x(x_0,v_0,t)]$ is equal to 1 for $x < 0$ and 0 otherwise, and $\theta_p = 1 - \theta_R$. The $\langle\cdot\rangle$ represents an average over initial condition. The escape rate is equal to the probability of the particle arriving at the barrier top multiplied by the probability of passing the saddle point; thus, we have the rate expression in an integral form,

$$k(t) = \int_{-\infty}^{\infty} v_0 W(0,v_0;t)\chi(v_0,t)dv_0, \tag{44}$$

where $W(0,v_0;t)$ is the possibility of the particle at the barrier top ($x = x_b = 0$) at time t, $\chi(v_0,t)$ is called the characteristic function or the passing probability over the saddle point. It is a number that is equal to one for reactive trajectories and zero for nonreactive trajectories. Mathematically, we have

$$\chi(v_0,t) = \int_0^{\infty} dx \int_{-\infty}^{\infty} dv W_b(x,v,t;0,v_0) = \int_0^{\infty} W_b(x,t)dx, \tag{45}$$

where $W_b(x,t)$ is the distribution of coordinate of the particle for the parabolic barrier case.

The potential used here consists of an inverse harmonic potential linking smoothing with a harmonic potential. It is of the form

$$U(x) = \begin{cases} \frac{1}{2}m\omega_0^2(x-x_0)^2, & x \leqslant x_c, \\ U_b - \frac{1}{2}m\omega_b^2 x^2, & x \geqslant x_c, \end{cases} \tag{46}$$

where x_c is the link point of two smooth potentials.

For the barrier passage process, it shows that the potential around the saddle point is $U(x) = -\frac{1}{2}m\omega_b^2 x^2$. The analytic solution for this parabolic barrier has the same form as for the harmonic potential, simply by substituting the frequency ω of the oscillator by $i\omega$. Then the characteristic function of the distribution $W_b(x,t)$ can be written as

$$\tilde{W}_b(k_1,t) = \exp(-ik_1\langle x(t)\rangle)\exp[-D|k_1|^{\mu} f(t)], \tag{47}$$

where

$$f(t) = \int_0^t |G_b(s)|^{\mu} ds, \tag{48}$$

$$G_b(t) = \frac{2e^{-\gamma t/2}}{m\sqrt{\gamma^2 + 4\omega_b^2}} \sinh\left(\frac{t\sqrt{\gamma^2 + 4\omega_b^2}}{2}\right), \tag{49}$$

$$\langle x(t)\rangle = \frac{2v_0 e^{-\gamma t/2}}{\sqrt{\gamma^2 + 4\omega_b^2}} \sinh\left(\frac{t\sqrt{\gamma^2 + 4\omega_b^2}}{2}\right) = v_0 G_b(t). \tag{50}$$

We express the solution $W_b(x,t)$ in terms of Fox's H function,

$$W_b(x,t) = W_0(x - \langle x(t)\rangle,t) = \frac{\pi}{\mu|x - \langle x(t)\rangle|} H_{2,2}^{1,1} \times \left[\frac{|x - \langle x(t)\rangle|}{(Df(t))^{\frac{1}{\mu}}} \middle| \begin{matrix}(1,1/\mu), & (1,1/2)\\ (1,1), & (1,1/2)\end{matrix}\right]. \tag{51}$$

Then the characteristic function $\chi(v_0,t)$ is written as

$$\chi(v_0,t) = \frac{1}{2} + \int_0^{\langle x(t)\rangle} W_0(x,t)dx. \tag{52}$$

With the transformation $v' = \frac{x}{G_b(t)}$, we rewrite $\chi(v_0,t)$ in another form,

$$\chi(v_0,t) = \frac{1}{2} + \int_0^{v_0} P(v',t)dv', \tag{53}$$

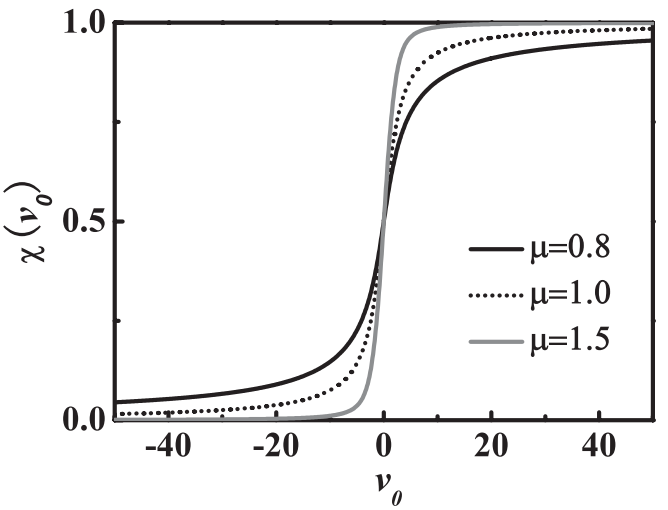

FIG. 8. Plot of the fractional reactivity index $\chi(v_0)$ [Eq. (55)] as a function of v_0 for various μ. The parameters used are $\gamma = 2.0$, $\omega_b^2 = 1.0$, $m = 1.0$, and $D = 1.0$.

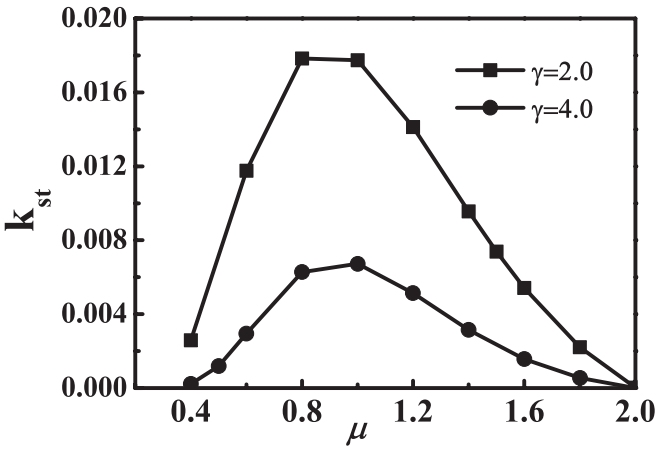

FIG. 9. The stationary escape rate as a function of the Lévy index μ. The parameters used are $\omega_0^2 = \omega_b^2 = 1.0$, $m = 1.0$, $D = 1.0$, and the barrier height $U_b = 4.0$.

where $P(v',t)$ is given by

$$P(v',t) = \frac{\pi}{\mu|v'|} H_{2,2}^{1,1}\left[\frac{|v'|}{(Df_b(t))^{\frac{1}{\mu}}}\begin{vmatrix}(1,1/\mu), & (1,1/2)\\ (1,1), & (1,1/2)\end{vmatrix}\right], \tag{54}$$

with $f_b(t) = \frac{f(t)}{|G_b(t)|^\mu}$. In the limit of $t \to \infty$, $f_b = \frac{2}{\mu m^\mu(\sqrt{\gamma^2+4\omega_b^2}-\gamma)}$. Thus, we obtain in the long time limit

$$\chi(v_0) = \frac{1}{2} + \int_0^{v_0} P(v')dv'. \tag{55}$$

The possibility of the particle arriving at the barrier top in Eq. (44) is taken as the stationary

$$W(0,v_0) = \frac{1}{(2\pi)^2}\int_{-\infty}^{\infty} dk_1 \int_{-\infty}^{\infty} dk_2 \cos(k_1 x_r)\cos(k_2 v_0) \times \exp\left[-D\int_0^{\infty} |k_1 G_x(t') + k_2 g_v(t')|^\mu dt'\right], \tag{56}$$

where $G_x(t) = c_0(t), g_v(t) = c_1(t)$, and x_r is the the bottom of the harmonic potential, in which the potential of the barrier top equals to $U_b = \frac{1}{2}m\omega_0^2 x_r^2$. Inserting Eqs. (55) and (56) into Eq. (44), we can calculate the stationary escape rate.

A plot of $\chi(v_0)$ as a function of v_0 is shown in Fig. 8. It is seen that the smaller the value of μ, the greater the region of $\chi(v_0)$ around $v_0 = 0$ that looks like $\frac{1}{2}$, which means more recrossing. When $v_0 > 0$, $\chi(v_0)$ decreases with the decrease of μ, strong diffusion is harmful for directional motion. When $v_0 < 0$, $\chi(v_0)$ increases with the decrease of μ, in this case, strong diffusion helps the the particle crossing over the barrier along the right direction.

Figure 9 shows the stationary rate constant calculated by Eq. (44) as a function of μ. Here the stationary rate constant does not depend monotonically on the Lévy index μ [18]. For large μ, the passing probability is also large; however, the stationary distribution becomes narrow, and thus the escape rate is small. On the other hand, for a small μ, the passing probability is small; however, the spatial distribution of the particles is wide. In this case, the rate constant is large. Therefore, there exists an optimal value of μ to make the escape rate become the maximum.

IV. CONCLUSION

We have investigated the inertial Lévy flight under the influence of several potential forces. The motion of particle is described by the Langevin equation with a general damping γ, which is subjected to a white Lévy noise of index μ. Especially for the case of linear and harmonic potentials, the probability density functions of the particle are derived by solving the fractional Fokker-Planck equation and the consequences under different physical parameters are analyzed in detail.

In the case of linear potential, there exists a transient contribution of the inertial term, which is negligible when the evolution time is much longer than the characteristic time γ^{-1}. The spatial distribution of the Lévy flight in the harmonic potential possesses infinite variance and its width is influenced by the inertial term for small γ. We have given the velocity distribution of the particle, which also has the stable Lévy shape. For the Lévy flight in a quartic potential with a given Lévy index $1 \leqslant \mu < 2$, there exists a transition from bimodal to unimodal shape for the distribution of coordinate as the damping coefficient decreases.

From the analytical expression of the escape rate of an inertial Lévy flight particle in a metastable potential presented here, we have found that the stationary escape rate is a nonmonotonic function of the Lévy index. This is due to the fact that the particles outside the barrier come back and interfere with themselves inside the barrier, so the strong diffusion such as Lévy flight does not lead to the large barrier escape.

ACKNOWLEDGMENTS

This work was supported by the National Natural Science Foundation of China under Grants No. 10875013 and No. 11175021 and the Specialized Research Foundation under Grant No. 20080027005.

APPENDIX A: SOLUTION OF $f(K,t)$

Letting $f(K,t) = \int_0^t g(K,t-s)ds$, we obtain the equation of $g(K,t-s)$ from Eq. (31),

$$\begin{aligned} &g(K,0) = m^{-\mu}|K|^\mu, \\ &\frac{\partial g(K,t-s)}{\partial t} - (\omega^2 K^2 - \gamma K + 1)\frac{\partial g(K,t-s)}{\partial K} = -\omega^2 \mu K g(K,t-s). \end{aligned} \tag{A1}$$

We expand $g(K,t-s)$ in the following way:

$$g(K,t-s)=\left|\sum_{i=0}^{n}c_i(t-s)K^i\right|^{\mu}. \tag{A2}$$

Substituting Eq. (A2) into Eq. (A1), we get the relations

$$\begin{aligned}
&c_1(0)=\frac{1}{m},\quad c_{i(i\neq 1)}(0)=0,\\
&\frac{\partial c_0(t-s)}{\partial t}-c_1(t-s)=0,\\
&\frac{\partial c_1(t-s)}{\partial t}-2c_2(t-s)+\gamma c_1(t-s)=-\omega^2 c_0(t-s),\\
&\vdots\\
&\frac{\partial c_{n-1}(t-s)}{\partial t}-nc_n(t-s)+\gamma(n-1)c_{n-1}(t-s)-\omega^2(n-2)c_{n-2}(t-s)=-\omega^2 c_{n-2}(t-s),\\
&\frac{\partial c_n(t-s)}{\partial t}+\gamma nc_n(t-s)-\omega^2(n-1)c_{n-1}(t-s)=-\omega^2 c_{n-1}(t-s),\\
&nc_n(t-s)=c_n(t-s).
\end{aligned} \tag{A3}$$

Taking account of the last equation of Eq. (A3) and introducing a new variable $t'=t-s$, we have

$$\begin{aligned}
&\frac{\partial c_0(t')}{\partial t'}-c_1(t')=0,\\
&\frac{\partial c_1(t')}{\partial t}+\gamma c_1(t')=-\omega^2 c_0(t'),\\
&c_2(t')=c_3(t')=\cdots=c_{n-1}(t')=c_n(t')=0.
\end{aligned} \tag{A4}$$

The Laplace transforms of $c_0(t')$ and $c_1(t')$ are given by

$$\hat{c}_0(p)=\frac{1}{m(p^2+\gamma p+\omega^2)},\quad \hat{c}_1(p)=\frac{p}{m(p^2+\gamma p+\omega^2)}. \tag{A5}$$

Based on the above relations, we have

$$\begin{aligned}
&c_0(t')=\frac{1}{m(\lambda_1-\lambda_2)}(e^{\lambda_1 t'}-e^{\lambda_2 t}),\quad c_1(t')=\frac{1}{m(\lambda_1-\lambda_2)}(\lambda_1 e^{\lambda_1 t}-\lambda_2 e^{\lambda_2 t'}),\quad \text{for}\quad \lambda_1\neq\lambda_2,\\
&c_0(t')=\frac{t'}{m}e^{\lambda_1 t'},\quad c_1(t')=\left(\frac{1}{m}+\frac{\lambda_1 t'}{m}\right)e^{\lambda_1 t'},\quad \text{for}\quad \lambda_1=\lambda_2,
\end{aligned} \tag{A6}$$

where $\lambda_{1,2}=-\frac{\gamma}{2}\pm\frac{\sqrt{\gamma^2-4\omega^2}}{2}$ are the eigenvalues of the equation $\lambda_0^2+\gamma\lambda_0+\omega^2=0$. Then $f(K,t)$ can be written as

$$f(K,t)=\int_0^t|c_0(t-s)+c_1(t-s)K|^{\mu}ds. \tag{A7}$$

APPENDIX B: NUMERICAL SIMULATION OF LANGEVIN EQUATION DRIVEN BY LÉVY NOISE

To obtain the probability distribution of particle in the quartic potential by simulating the trajectories from Eq. (1), the stochastic Euler algorithm is applied. To this end, the Langevin equation driven by white Lévy noise is discretized in time as

$$\begin{aligned}
&x(t+\triangle t)=x(t)+v(t)\triangle t,\\
&v(t+\triangle t)=v(t)-\gamma v(t)\triangle t+\frac{F(x)}{m}\triangle t+\frac{(D\triangle t)^{\frac{1}{\mu}}}{m}\xi_{\mu}.
\end{aligned} \tag{B1}$$

Here we use a more convenient method proposed by Chambers, Mallows, and Stuck [19,20] to generate symmetric Lévy μ-stable random number:

$$\xi_{\mu}=\left(\frac{-\ln u\cos\phi}{\cos[(1-\mu)\phi]}\right)^{(1-1/\mu)}\frac{\sin(\mu\phi)}{\cos\phi}, \tag{B2}$$

where $\phi=\pi(\nu-1/2)$ and $u,\nu\in(0,1)$ are independent uniform random numbers.

[1] H. Scher and E. W. Montroll, Phys. Rev. B **12**, 2455 (1975).
[2] I. Y. Wong, M. L. Gardel, D. R. Reichman, E. R. Weeks, M. T. Valentine, A. R. Bausch, and D. A. Weitz, Phys. Rev. Lett. **92**, 178101 (2004).
[3] E. Barkai, Phys. Rev. Lett. **90**, 104101 (2003).
[4] G. Zumofen, J. Klafter, and A. Blumen, J. Stat. Phys. **65**, 991 (1991).
[5] H. C. Fogedby, Phys. Rev. E **50**, 1657 (1994).
[6] W. R. Schneider and W. Wyss, J. Math. Phys. **30**, 134 (1989).
[7] A. Ott, J. P. Bouchaud, D. Langevin, and W. Urbach, Phys. Rev. Lett. **65**, 2201 (1990).
[8] G. Zumofen and J. Klafter, Phys. Rev. E **51**, 2805 (1995).
[9] G. M. Viswanathan, V. Afanasyev, S. V. Buldyrev, E. J. Murphy, P. A. Prince, and H. E. Stanley, Nature (London) **381**, 413 (1996).
[10] S. Jespersen, R. Metzler, and H. C. Fogedby, Phys. Rev. E **59**, 2736 (1999).
[11] H. Katori, S. Schlipf, and H. Walther, Phys. Rev. Lett. **79**, 2221 (1997).
[12] A. V. Chechkin, J. Klafter, V. Y. Gonchar, R. Metzler, and L. V. Tanatarov, Phys. Rev. E **67**, 010102(R) (2003).
[13] B. J. West and V. Seshadri, Physica A **113**, 203 (1982).
[14] A. V. Chechkin, V. Y. Gonchar, and M. Szydlowski, Phys. Plasmas **9**, 78 (2002).
[15] E. Lutz, Phys. Rev. Lett. **86**, 2208 (2001).
[16] D. J. Tannor and D. Kohen, J. Chem. Phys. **100**, 4932 (1994).
[17] D. Kohen and D. J. Tannor, J. Chem. Phys. **103**, 6013 (1995).
[18] J. D. Bao, H. Y. Wang, Y. Jia, and Y. Z. Zhuo, Phys. Rev. E **72**, 051105 (2005); J. D. Bao, J. Chem. Phys. **124**, 114103 (2006).
[19] J. M. Chambers, C. L. Mallows, and B. W. Stuck, J. Am. Stat. Assoc. **71**, 340 (1976).
[20] D. Fulger, E. Scalas, and G. Germano, Phys. Rev. E **77**, 021122 (2008).